Target Localization and Tracking From Doppler-Shift Measurements

YIU-TONG CHAN, SENIOR MEMBER, IEEE, AND FREDERICK L. JARDINE

Abstract—**It is possible to localize a moving source which is nonmaneuvering and radiates a constant frequency tone from measurements of the Doppler-shifted frequency at several sensors. Due to the nonlinear nature of the problem, it is necessary to find the solution by grid searches. However, if measurements of the rates of frequency changes are available, the search is only in three dimensions instead of the normal five in source frequency, its *x-y* positions, and speeds.**

The validity of the new localization scheme of combining frequency and frequency-rate measurements is confirmed with simulation studies. The overall system includes a least-squares track-sort algorithm to differentiate the true track from the extraneous track, and a Kalman tracker for the prediction of future source positions so as to reduce the grid search size. An error analysis relating localization accuracy to uncertainties in frequency measurements and sensor positions is also given.

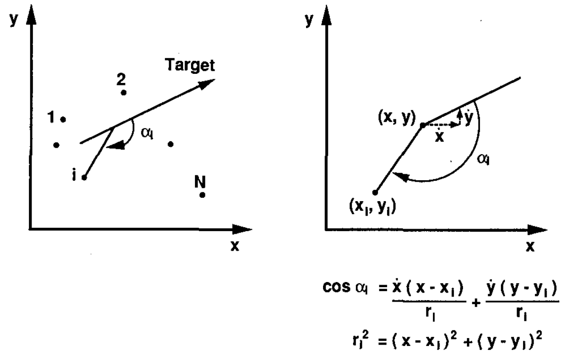

Fig. 1. Localization geometry.

I. INTRODUCTION

A METHOD of determining the position and velocity of a moving object which radiates a tone is by the measurements of the Doppler-shifted frequencies at several separate locations. Two application examples are in passive sonar, where sonobuoys intercept the acoustic energy radiating from a moving source for detection and localization [1], and in the tracking of a projectile which emits a tone [2], [3]. As depicted in Fig. 1, a constant-course and speed target is moving in a field of N sensors and emitting a constant tone of frequency f_0. The sensors' placement pattern can be random, but their positions are known. Because of the Doppler shift, each sensor measures a different frequency. Localization of the target is the determination, at a given instant of time, of the target parameter vector $s = (x, y, \dot{x}, \dot{y})$, where x, y and $\dot{x}$, $\dot{y}$ are, respectively, the position and velocity coordinates of the target.

Depending upon practical constraints and available information, there are many variations of this problem. As shown in (1) below, the frequency measurements are related to the elements of S via f_0. Thus when f_0 is not known, for example, in passive sonar, at least five sensors are needed to give five independent frequency measurements to solve for f_0 and the vector S [4]. Often the number of sensors in simultaneous contact with the target may be less and the localization has to be performed over several measurement periods [2]. If f_0 is known, for example, in radar tracking [5], [6], then a single sensor with three sequential frequency measurements is sufficient to localize the target. However, in [5], [6] the target parameter vector contains only three terms: range, velocity, and the angle between them. Without an *a priori* knowledge of the target bearing, this three-element vector cannot specify uniquely the target position with respect to the sensor. Yet another application is reported in [3], where the target velocity is assumed to be known and the desired parameters are f_0 and the minimal distance between the target and sensor.

Since (1) below is a nonlinear equation, most solution methods [2], [3], [5] are iterative, choosing successive values of S to minimize a cost function. The exception is [6], where an exact solution is given. But as mentioned earlier, the approach in [6] is valid only when f_0 is known and can give only estimates of target range, velocity, and the angle between them, but not the relative bearing of target to sensor. We present in this paper a new method of passive localization based on the measurements of Doppler shifts. It has applications in underwater acoustics, and although it requires a grid search, the search dimension is three instead of five. As will be shown in Section II, by introducing the variable of frequency rate into the Doppler equation, the unknowns $\dot{x}$ and $\dot{y}$ are eliminated. The same section also describes the proposed localization-tracking system. An analysis of the sensitivity of the localization to accuracy in the measurements is provided in Section III. Section IV contains the simulation results, and Section V, the conclusions.

Manuscript received September 5, 1989; revised February 20, 1990. This work was partially supported by the Defence Research Establishment Atlantic.

Y.-T. Chan is with the Department of Electrical and Computer Engineering, Royal Military College of Canada, Kingston, ON K7K 5L0, Canada.

F. L. Jardine was with the Department of Electrical and Computer Engineering, Royal Military College of Canada, Kingston, ON K7K 5L0, Canada. He is now with the Directorate of Maritime Combat Systems, National Defence Headquarters (Canada).

IEEE Log Number 9036131.

II. PROBLEM FORMULATION AND SOLUTION

A. The Doppler Equation with $\dot{f}$

Referring to Fig. 1, an underwater target is moving on a constant-course and speed (V) track and radiating a tone

0364-9059/90/0700-0251$01.00

of constant frequency f_0. The N sensors, $1, \cdots, N$ intercept a Doppler-shifted version of the tone so that the ith sensor measures a frequency:

$$f_1 = f_0 \left(1 + \frac{V \cos \alpha_i}{C}\right) \tag{1}$$

where C is the speed of sound in water. Normally, a frequency line tracker (FLT) [1], [7], [8] processes each sensor output to give estimates of f_i and $\dot{f}_i$, the rate of change of f_i. Typically, an FLT [8] determines f_i by a spectral analysis of the received signal and uses these f_i as input to a tracker (for example, Kalman), which then produces smoothed estimates of f_i as well as $\dot{f}_i$. After each measurement period, there are available f_i, $i = 1, \cdots, N$, from which the unknowns $s = (x, y, \dot{x}, \dot{y})$ are to be determined via (1).

Although f_0 is not required specifically for localization, it is nevertheless an additional unknown in (1) and therefore at least five sensors are needed to ensure observability; i.e., a determinant solution. In practice, having five sensors in simultaneous contact with a target is rare, and often it is necessary, with fewer in-contact sensors, to perform the localization over several measurement periods. Alternatively, by introducing $\dot{f}_i$, which is an additional measurement, four sensors in contact are sufficient to give an instantaneous localization. Of course, it can easily be argued that since an FLT can provide $\dot{f}_i$ only after at least two measurements of f_i, using $\dot{f}_i$ is thus equivalent to localization over two measurements periods. However, thee more important issue here is that at any instant when f_i and $\dot{f}_i$ are available, present localization schemes, which do not make use of $\dot{f}_i$, will still require five sensors for instantaneous localization. As the following will show, by developing a relationship between $\dot{f}_i$ and the three unknowns, only four sensors are needed for instantaneous localization.

Differentiating (1) with respect to time yields:

$$\dot{f}_i = -f_0 \dot{\alpha}_i \frac{V}{C} \sin \alpha_i. \tag{2}$$

Since the angular speed,

$$\dot{\alpha}_i = \frac{V \sin \alpha_i}{r_i} \tag{3}$$

it follows from (2) and (3) that

$$V^2 \sin^2 \alpha_i = -\frac{C r_i \dot{f}_i}{f_0}. \tag{4}$$

It is also easy to obtain, from (1):

$$V^2 \cos^2 \alpha_i = \frac{C^2 (f_i - f_0)^2}{f_0^2}. \tag{5}$$

Summing (4) and (5) eliminates α_i and gives:

$$V^2 = K_i + M_i \tag{6}$$

where

$$K_i = \frac{C^2 (f_i - f_0)^2}{f_0^2} \tag{7}$$

and

$$M_i = -\frac{C \dot{f}_i [(x - x_i)^2 + (y - y_i)^2]^{1/2}}{f_0}. \tag{8}$$

In (8), (x, y) and (x_i, y_i) are the coordinates of the target and the ith sensor, respectively. The problem is to find, from the measurements $f_i, \dot{f}_i$, $i = 1, \cdots, N$, the unknowns V, x, y, and f_0. Note that by using

$$V^2 = \dot{x}^2 + \dot{y}^2 \tag{9}$$

and introducing $\dot{f}_i$, the derivation above serves to reduce the unknowns from five to four.

The solution of (6) is by grid search, but only in the variables x, y, f_0. There is no need to include V in the search, since it is a function of K_i and M_i in (6) and is a constant for all i. Let the grid search cost function be:

$$J = \sum_{i=1}^{N} (V^2 - K_i - M_i)^2. \tag{10}$$

Setting the partial derivative of J with respect to V^2 to zero and solving for V^2 gives:

$$V^2 = \frac{\Sigma K_i + \Sigma M_i}{N}. \tag{11}$$

For convenience, the summation limits in (11) and the equations following are suppressed but understood to be from 1 to N. Substituting (11) into (10) produces:

$$J = \Sigma \left(\frac{\Sigma K_i + \Sigma M_i}{N} - K_i - M_i \right)^2 \tag{12}$$

and normalizing each term in the summation in (12) yields the final cost function:

$$J_0 = \Sigma \left[1 - \frac{\frac{\Sigma K_i + \Sigma M_i}{N}}{K_i + M_i} \right]^2. \tag{13}$$

The normalization process simply changes the absolute deviations in (12) to fractional deviations in (13).

The grid search strategy is to evaluate, for each grid point (x, y, f_0), the cost J_0 in (13) and choose the grid point which gives the minimum J_0 as the solution. In a practical situation, much additional information is available to limit the grid size and grid resolution to reasonable values. In sonar, the grid size is at most a few km on a side at the beginning of a track, and as the track develops, the area will decrease as determined by the prediction variance of the tracker. As for the grid resolution, it need not be much smaller than the tolerance limits on the position accuracy of a sensor. The maximum speed of a target is also normally known, so that the range of Doppler shifts is easily computed from (1), for $\cos \alpha_i = \pm 1$, which in turn limits the search range for f_0. Indeed, if f_0 can be obtained from a closest point-of-approach measurement, then the grid search reduces to two dimensions. In any event, f_0 can usually be determined to within 1% from the f_i [9]. Thus the grid size for solving (13) is quite manageable.

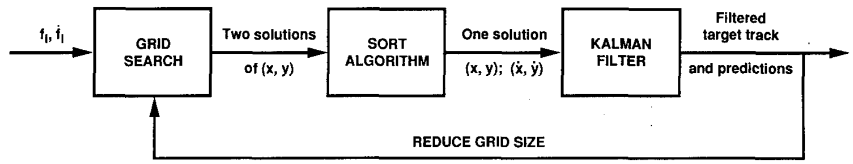

Fig. 2. The localization-tracking system.

B. Track Sorting

Due to uncertainties (for example, in sensor positions and the measurements f_i and the nonuniqueness of the solution of a nonlinear equation) the (x, y, f_0) that minimizes J_0 is not always the correct solution. Instead, the correct solution may have a J_0 slightly above the minimum. To avoid missing the correct solution, it has been found necessary to include five grid points that give the five lowest J_0. From those five points, two cluster points, based on dispersions from the centers, are formed and entered into a track sort algorithm. This algorithm distinguishes the correct solution from the erroneous one by relying on the nonmaneuvering target assumption. This scheme is *ad hoc*. Certainly, there is no guarantee that the correct solution is always among the five chosen grid points, especially under noisy conditions. There will also be more accuracy if the track sort algorithm takes all five grid points instead of two clustered points. The above choices are simply made to reduce the computations, but at the same time are found not to compromise the performance significantly in the simulation.

The sort algorithm selects a sequence of points $(x(n), y(n))$, where n is the time index, to minimize:

$$J_s = J_x + J_y \tag{14}$$

where

$$J_x = \sum_{n=k}^{k+M} [x(n) - nT\dot{x} - b_x]^2 \tag{15}$$

and

$$J_y = \sum_{n=k}^{k+M} [y(n) - nT\dot{y} - b_y]^2. \tag{16}$$

In (15) and (16), T is the known time interval between nT and $(n+1)T$; $\dot{x}$, $\dot{y}$ are the unknown speed coordinates; and b_x and b_y are the unknown intercepts. Given a set of $x(n)$, $n = k, \cdots, k+M$, the $\dot{x}$ and b_x that best fit (15) is given by the least-squares solution,

$$\begin{bmatrix} \dot{x} \\ b_x \end{bmatrix} = \Lambda^{-1} \begin{bmatrix} T\Sigma x(n) \\ \Sigma x(n) \end{bmatrix} \tag{17}$$

where

$$\Lambda = \begin{bmatrix} T\Sigma n^2 & T\Sigma n \\ T\Sigma n & N+1 \end{bmatrix}. \tag{18}$$

The summation limits in (17) and (18) are from k to $k+M$. The equations for $\dot{y}$ and b_y are similar.

After finding $\dot{x}$, $\dot{y}$ and b_x and b_y, the residual J_s is then evaluated for the sequence $(x(n), y(n))$. The sequence with the least residual is the one which best fits the constant $\dot{x}$, $\dot{y}$ assumption. As there are two solutions of $(x(n), y(n))$ that enter into the algorithm at each n, the number of sequences to check is 2^L, after L measurement intervals. To save computations, the following procedure is used: Initially, the algorithm waits for five intervals and then checks the $2^5 = 32$ possible sequences. It retains only the two sequences that possess the lowest J_s. At the sixth interval, two more input points arrive. Each of them is checked with the retained sequence, requiring the computation of four J_s. Again, only two sequences with the lowest J_s are kept. This process continues until the relative magnitudes of the two lowest J_s are sufficiently disparate; i.e., when

$$\frac{J_s\,(\text{minimum}) - J_s\,(\text{next minimum})}{J_s\,(\text{minimum})} \geq \text{Threshold}. \tag{19}$$

From then on there is only a single sequence of target positions, which the sort algorithm uses to eliminate one of the two input points. The sort algorithm performs no filtering functions. Its output is filtered by a Kalman tracker, which also gives predictions of future target positions, allowing a narrowing of the grid size as the track progresses. Fig. 2 is a block diagram of the localization-tracking system.

III. Variance Analysis

In practice, there are many sources of errors in the localization by Doppler-shift measurements. Aside from possible violations of the basic assumptions of a constant f_0 and a nonmaneuvering source, errors in the measurements f_i, $\dot{f}_i$ and in the sensor positions x_i, y_i also contribute to the overall inaccuracies in the target parameter estimation. A complete study of all the factors and their influence on the estimation accuracy is given in [10]. We outline here the methodology, and give a numerical example in Section IV.

The goal is to find an expression which relates a standard deviation (SD) in x (or y) to an SD in other variables. To this end, it is necessary to consider the intermediate variable, range r_i, which comes from a rewriting of (6):

$$r_i = [(x - x_i)^2 + (y - y_i)^2]^{1/2} = \frac{C(f_i - f_0)^2}{f_0 \dot{f}_i} - \frac{f_0 V^2}{C \dot{f}_i}. \tag{20}$$

Thus the range SD as a function of the SD of a particular variable is easily found by taking the partial derivative of r_i with respect to that variable, evaluating the partials at the nominal values, and multiplying it by the SD of the variable in question. The sum of all these individual-range SD's then gives the total-range SD.

From r_i and known x_i, y_i, (x, y) is found by the minimiza-

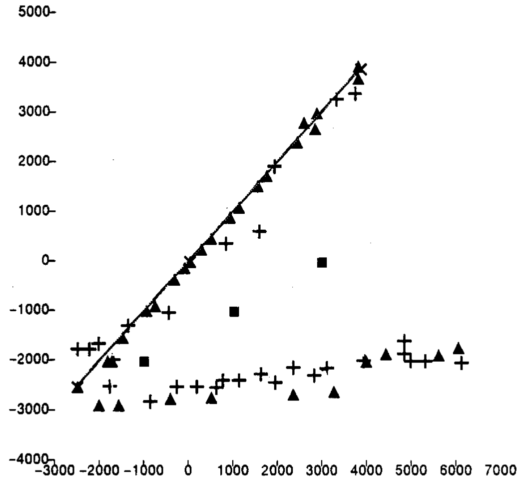

Fig. 3. Plot of grid-search solutions—three sensors, linear placement. (+) and (▲) = solution points. (■) = sensors.

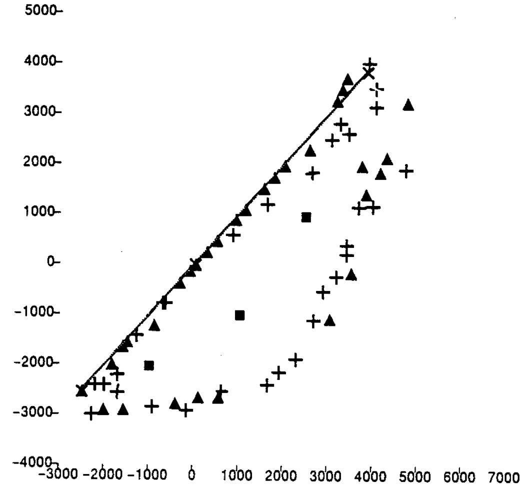

Fig. 4. Plot of grid-search solutions—three sensors, off-linear placement. (+) and (▲) = solution points. (■) = sensors.

tion of the cost function,

$$L = \sum_{i=1}^{N} g_i^2 \tag{21}$$

where

$$g_i = r_i^2 - (x - x_i)^2 - (y - y_i)^2. \tag{22}$$

The solution is found by setting the partial derivatives of L with respect to x, y to zero; i.e.,

$$\Sigma g_i(x - x_i) = 0 \tag{23}$$

$$\Sigma g_i(y - y_i) = 0. \tag{24}$$

By taking the total differentials of (23) and (24) and after some algebra, expressions are obtained that relate an SD in x and y, together with the covariance of x and y, to the nominal values of r_i, x_i, y_i and their respective SD's. Details are contained in the Appendix.

IV. Simulation Results

In the simulation studies the source is moving at a constant speed of $V = 10$ m/s, at a constant bearing of 45°, and radiates at $f_0 = 150$ Hz. Its starting position is at (−2500, −2500 m). The frequency measurement interval is $T = 30$ s and each sensor takes a total of 30 measurements, so that the tracking process lasts for 900 s. At the end of the track, the source is at (3863, 3863 m). From (1), letting $C = 1500$ m/s, it is easily calculated that the maximum Doppler shift is ± 1 Hz. The initial (first five measurements) grid size is 20×20 km, centered at (0, 0), and the grid points are 150×150 m apart. From the sixth measurement onward, the grid is centered at the position predicted by the Kalman filter, and the grid size is reduced to an area determined by the SD of the prediction.

Various sensor placement configurations were studied. If f_0 is known, three sensors are sufficient to localize, and Figs. 3 to 6 are plots of the solution points (the sort algorithm is not in operation yet), showing two solution points per measurement.

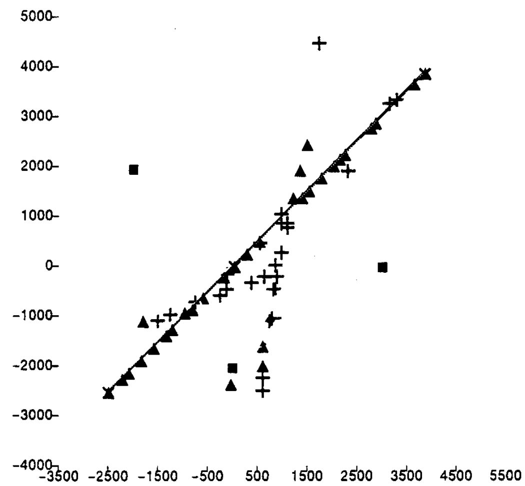

Fig. 5. Plot of grid-search solutions—three sensors, track-straddled. (+) and (▲) = solution points. (■) = sensors.

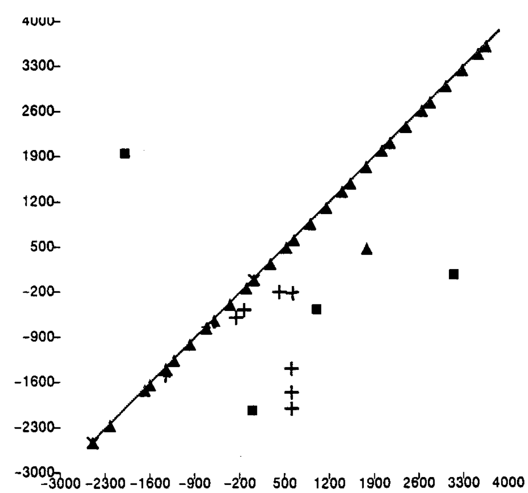

Fig. 6. Plot of grid search solutions—four sensors. (+) and (▲) = solution points. (■) = sensors.

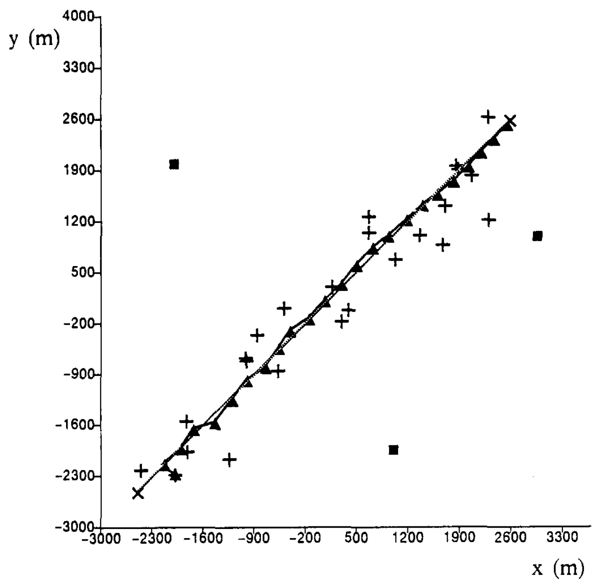

Fig. 7. Sample tracking run. (+) = noisy inputs. (▲) = Kalman estimates. (■) = sensors.

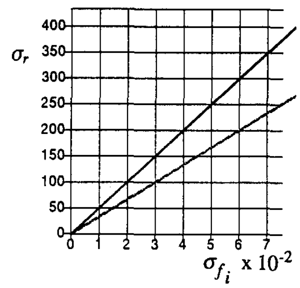

Fig. 8. Sensitivity to errors in f_i.

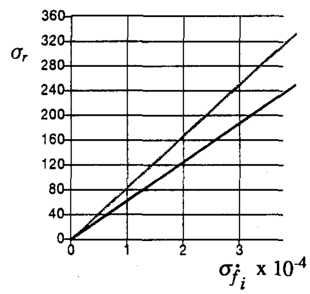

Fig. 9. Sensitivity to errors in $\dot{f}_i$.

TABLE I
SUMMARY OF SD

σ_r	σ_s	σ_x	σ_y
100	50	173	177
200	100	347	354
300	100	491	500
400	100	640	652

These are denoted by crosses and triangles. The straight solid line denotes the true track. In Fig. 3 the sensors, denoted by solid squares, are in a straight line, and it is obvious that a ghost track exists on the opposite side of the sensor line. In this sensor configuration even the sort algorithm will not be able to eliminate the ghost track, since it will also satisfy the constant track test. To avoid this ambiguous situation, there should not be a linear placement of sensors. In Fig. 4 the sensors are off the linear pattern and the ghost track becomes curved, which the sort algorithm can easily eliminate. When the track straddles the sensors, as is the case in Fig. 5, the ghost and true tracks cross each other, but it is still possible to eliminate the ghost track. When four sensors are present there is added redundancy. As a result, in many instances the five solution points cluster into a single point, so that only a few ghost solutions are present in the track in Fig. 6. Finally, the effectiveness of the overall localization-tracking system is demonstrated in Fig. 7. The true track is the straight line, the Kalman estimates are the triangles, and the crosses are the noisy inputs from the sort algorithm to the Kalman tracker. The SD's of f_i and $\dot{f}_i$ combined to give an SD in r_i of 400. These SD's are reasonable in that they are within the accuracy of FLT's.

Next, the effects of the inaccuracies in various parameters on localization are studied. Figs. 8 and 9 are plots of an SD ranged against an SD in f_i and $\dot{f}_i$. There are two lines in each figure, with the darker line denoting measurements at the closest point-of-approach and the other at $\alpha = 60°$. Table I is a summary of the SD in x and y, denoted by σ_x and σ_y, respectively, as a function of the SD in σ_r and σ_s, the range and sensor position SD's. In the calculation the nominal values are: Source at (−3000, 2000), and three sensors at (0, 0), (−2000, 0), and (2000, 0). It is assumed that the x–y errors in the sensor positions are uncorrelated.

V. Conclusions

This paper has described a novel solution to the localization-by-Doppler-measurements problem. By using the rate of frequency change, the number of unknowns is reduced from five to four and the solution of the nonlinear equation to a three-dimensional search. The nonlinear localization equation gives rise to nonunique solutions, and a sort algorithm was devised to eliminate the wrong solutions as the track progresses. Simulation results have confirmed the validity of the scheme and an analysis on the relationship between the accuracy of the localization and other measurement parameters is also given.

Appendix

Variance Analysis

This appendix develops the expressions that give the position variances σ_x^2, σ_y^2 in terms of variances of the other variables. The key equation is (20), rewritten here with the subscript i deleted for convenience:

$$r = \frac{C(f - f_0)^2}{f\dot{f}_0} - \frac{f_0 V^2}{C\dot{f}}. \tag{A1}$$

Due to measurement errors and parameter variations, all variables in (A1) will contain a mean (or nominal) value plus a noise component. Let

$$f_0 = \bar{f}_0 + \epsilon_{f_0} \tag{A2}$$

where the bar denotes the mean value in this appendix, and ϵ_{f_0}, a zero-mean random variable (ZMRV), denotes the uncertainties in f_0. Substitution of (A2) into (1) yields:

$$f = \bar{f} + \left(1 + \frac{\bar{V}\cos\bar{\alpha}}{\bar{C}}\right)\epsilon_{f_0} + \epsilon_f \tag{A3}$$

where

$$\bar{f} = \bar{f}_0\left(1 + \frac{\bar{V}\cos\bar{\alpha}}{\bar{C}}\right) \tag{A4}$$

and the uncertainties in V, C, and α are assumed to have negligible effects on f, since

$$1 \gg \frac{V\cos\alpha}{C}$$

in most situations. The ZMRV ϵ_f denotes the measurement error in f and is independent of ϵ_{f_0}. The frequency rate is

$$\dot{f} = \bar{\dot{f}} + k_1\epsilon_f + k_2\epsilon_{f_0} + \epsilon_{\dot{f}} \tag{A5}$$

where k_1 and k_2 are constants that account for the degree to which ϵ_f and ϵ_{f_0} affect $\dot{f}$, and $\epsilon_{\dot{f}}$ is a ZMRV denoting the measurement errors in $\dot{f}$. Note that in the manner in which they are defined, ϵ_f, ϵ_{f_0}, and $\epsilon_{\dot{f}}$ are independent.

The variance of r is given by the approximation [11]:

$$\sigma_r^2 \simeq \left(\frac{\partial r}{\partial c}\right)^2\sigma_c^2 + \left(\frac{\partial r}{\partial V}\right)^2\sigma_v^2 + \left(\frac{\partial r}{\partial \epsilon_f}\right)^2\sigma_{\epsilon_f}^2 + \left(\frac{\partial r}{\partial \epsilon_{\dot{f}}}\right)^2\sigma_{\epsilon_{\dot{f}}}^2 + \left(\frac{\partial r}{\partial \epsilon_{f_0}}\right)^2\sigma_{\epsilon_{f_0}}^2 \tag{A6}$$

where all partial derivatives are evaluated at the mean values of the variables. The partial derivatives are:

$$\frac{\partial r}{\partial C} = \left(\frac{f - f_0}{\dot{f}f}\right)^2 - \frac{f_0V^2}{C^2\dot{f}} \tag{A7}$$

$$\frac{\partial r}{\partial V} = -\frac{2f_0V}{C\dot{f}} \tag{A8}$$

$$\frac{\partial r}{\partial \epsilon_f} = \frac{C}{f_0\dot{f}}[2\dot{f}(f - f_0) - (f - f_0)^2k_1] + \frac{f_0V^2k_1}{C\dot{f}} \tag{A9}$$

$$\frac{\partial r}{\partial \epsilon_{\dot{f}}} = \frac{1}{\dot{f}^2}\left[\frac{f_0V^2}{C} - \frac{C(f - f_0)^2}{f_0}\right] \tag{A10}$$

$$\frac{\partial r}{\partial \epsilon_{f_0}} = \frac{2Cf_0\dot{f}(f - f_0)\left(\frac{V}{C}\cos\alpha\right) - C(f - f_0)^2(f_0k_2 + \dot{f})}{(f_0\dot{f})^2} - \frac{V^2(f - f_0k_2)}{C\dot{f}^2}. \tag{A11}$$

Now that σ_r^2 is found, the localization variances are next obtained as a function of σ_r^2 and the sensor position variances $\sigma_{x_i}^2$ and $\sigma_{y_i}^2$ from (23) and (24) in the text. Taking the total differentials of (23) gives:

$$\Sigma g_i dx - \Sigma g_i dx_i + \Sigma x dg_i - \Sigma x_i dg_i = 0. \tag{A12}$$

It is assumed that with the mean values, $g_i \equiv 0$ for all i, i.e., the localization estimate is unbiased, so that (A12) simplifies to:

$$x\Sigma dg_i = \Sigma x_i\, dg_i. \tag{A13}$$

Let

$$\Delta x_i = \bar{x} - \bar{x}_i, \qquad \Delta y_i = \bar{y} - \bar{y}_i \tag{A14}$$

and after some algebra, (A13) becomes:

$$dx\,\Sigma\,\Delta x_i^2 + dy\,\Sigma\,\Delta x_i\,\Delta y_i = N_1 \tag{A15}$$

where

$$N_1 = \Sigma r_i\,\Delta x_i dr_i + \Sigma\,\Delta x_i^2\,dx_i + \Sigma\,\Delta x_i\,\Delta y_i dy_i. \tag{A16}$$

Repeating the same operations on (24) results in:

$$dy\,\Sigma\,\Delta y_i^2 + dx\,\Sigma\,\Delta y_i\,\Delta x_i = N_2 \tag{A17}$$

where

$$N_2 = \Sigma r_i\,\Delta y_i dr_i + \Sigma\,\Delta y_i^2 dy_i + \Sigma\,\Delta y_i\,\Delta x_i dx_i. \tag{A18}$$

Solving (A15) and (A17) gives:

$$dx = \frac{N_1\Sigma\,\Delta y_i^2 - N_2\Sigma\,\Delta x_i\,\Delta y_i}{D} \tag{A19}$$

and

$$dy = \frac{N_2\Sigma\,\Delta x_i^2 - N_1\Sigma\,\Delta y_i\,\Delta x_i}{D} \tag{A20}$$

where

$$D = (\Sigma\,\Delta x_i^2)(\Sigma\,\Delta y_i^2) - (\Sigma\,\Delta x_i^2\,\Delta y_i)^2. \tag{A21}$$

Next, the following terms are evaluated:

$$\sigma_x^2 = E[(dx)^2] \tag{A22}$$

$$\sigma_y^2 = E[(dy)^2] \tag{A23}$$

$$\sigma_{xy} = E[(dx)(dy)] \tag{A24}$$

where $E[\cdot]$ is the expectation operator. In computing (A23) and (A24), it is assumed that

$$x_i = \bar{x}_i + \epsilon_{x_i} \tag{A25}$$

$$y_i = \bar{y}_i + \epsilon_{y_i} \tag{A26}$$

$$r_i = \bar{r}_i + \epsilon_{r_i} \tag{A27}$$

and that ϵ_{x_i}, e_{y_i}, and ϵ_{r_i} are independent ZMRV, and

$$\sigma_r^2 = E\{\epsilon_{r_i}^2\}$$

is available from (A6). To obtain (A23) and (A24), the necessary terms are:

$$E[N_1^2] = \Sigma r_i^2\,\Delta x_i^2 \sigma_{r_i}^2 + \Sigma\,\Delta x_i^4 \sigma_{x_i}^2 + \Sigma\,\Delta x_i^2\,\Delta y_i^2 \sigma_{y_i}^2 \quad \text{(A28)}$$

$$E[N_2^2] = \Sigma r_i^2\,\Delta y_i^2 \sigma_{r_i}^2 + \Sigma\,\Delta y_i^4 \sigma_{y_i}^2 + \Sigma\,\Delta x_i^2\,\Delta y_i^2 \sigma_{x_i}^2 \quad \text{(A29)}$$

and

$$E[N_1 N_2] = \Sigma r_i^2\,\Delta x_i\,\Delta y_i \sigma_{r_i}^2 + \Sigma\,\Delta x_i^3\,\Delta y_i \sigma_{x_i}^2 + \Sigma\,\Delta x_i\,\Delta y_i^3 \sigma_{y_i}^2. \quad \text{(A30)}$$

To summarize, given the mean values of V, C, f_0, f_i, $\dot{f}_i$, x_i, and y_i and their respective variances

$$\sigma_v^2,\ \sigma_c^2,\ \sigma_{\epsilon f_0}^2,\ \sigma_{\epsilon f}^2,\ \sigma_{\epsilon \dot{f}}^2,\ \sigma_{x_i}^2,\ \sigma_{y_i}^2$$

and k_1, k_2, we first compute σ_r^2 from (A6) and then σ_x^2, σ_y^2, and σ_{xy} from (A22)-(A24).

Acknowledgment

The authors wish to thank Drs. A. Ashley and M. McIntyre of the Defence Research Establishment Atlantic for many fruitful discussions.

References

[1] R. E. Bethel and J. A. Gauss, "A Bayesian approach to frequency line tracking," in *Proc. IEEE EASCON*, 1981, pp. 286-290.

[2] E. Weinstein and N. Levanon, "Passive array tracking of a continuous wave transmitting projectile," *IEEE Trans. Aerosp. Electron. Syst.*, vol. AES-16, Sept. 1980, pp. 721-726.

[3] J. K. Statman and E. R. Rodemich, "Parameter estimation based on Doppler frequency shifts," *IEEE Trans. Aerosp. Electron. Syst.*, vol. AES-23, Jan. 1987, pp. 31-39.

[4] P. M. Schultheiss and E. Weinstein, "Estimation of differential Doppler shifts," *J. Acoust. Soc. Amer.*, vol. 66, no. 5, Nov. 1979, pp. 1412-1419.

[5] N. Levanon, "Some results from utilizing Doppler derivatives," *IEEE Trans. Aerosp. Electron. Syst.*, vol. AES-16, Sept. 1980.

[6] R. J. Webster, "An exact trajectory solution from Doppler shift measurements," *IEEE Trans. Aerosp. Electron. Syst.*, vol. AES-18, Mar. 1982, pp. 249-252.

[7] F. M. Hsu and A.A. Giordano, "Line tracking using autoregressive spectral estimates," *IEEE Trans. Acoust., Speech, Signal Processing*, vol. ASSP-25, pp. 510-519, Dec. 1977.

[8] J. R. Williams and G. G. Ricker, "Digital line trackers," Interstate Electron. Corp., Anaheim, CA, IEC Tech. Note 4800-6-6, Dec. 1971.

[9] J. A. Fawcett, "TMA performance for towed arrays of low maneuverability," in *Underwater Acoustic Data Processing* (NATO ASI Series E, vol. 161), Y. T. Chan, Ed. Boston, MA: Kluwer, 1989.

[10] F. L. Jardine, "Localization and tracking of narrowband sources," M.Eng. thesis, Dept. of Comp. Elec. Eng., Royal Military College of Canada, Kingston, ON, May 1989.

[11] A. Papoulis, *Probability, Random Variables, and Stochastic Processes*. New York: McGraw-Hill, 1984.

★

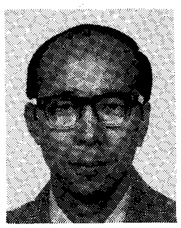

Yiu-Tong Chan (SM'80) was born in Hong Kong. He received the B.Sc. and M.Sc. degrees from Queen's University, Kingston, ON, Canada, in 1963 and 1967, respectively, and the Ph.D. degree from the University of New Brunswick, Fredericton, in 1973, all in electrical engineering.

He has worked with Northern Telecom Ltd. and Bell-Northern Research. Since 1973 he has been at the Royal Military College of Canada, Kingston, ON, where he is presently a Professor. His research interests are in sonar signal processing and passive localization and tracking techniques, and he has served as a Consultant on sonar systems. He was an Associate Editor (1980-1982) of the IEEE Transactions on Acoustics, Speech, and Signal Processing and was the Technical Program Chairman of the 1984 International Conference on Acoustics, Speech, and Signal Processing (ICASSP'84). He directed the NATO Advanced Study Institute on Underwater Acoustic Data Processing in 1988 and is the General Chairman of ICASSP'91, to be held in Toronto, ON, Canada.

★

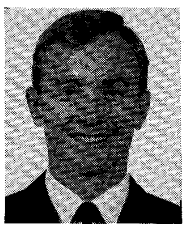

Frederick L. Jardine graduated from the Royal Military College of Canada in 1980 with the B.Eng. degree in electrical engineering. Upon graduation he was commissioned in the Canadian Navy and served in Maritime Combat Systems Engineering positions at sea and on-shore. In 1989 he completed the M.Eng. degree, also at the Royal Military College. He is currently serving in the Directorate of Maritime Combat Systems in the National Defence Headquarters as a Sonar Systems Project Engineer.